High resolution mass approach to characterize refrigerated black truffles stored under different storage atmospheres

Food Research International xxx (2017) xxx-xxx

Contents lists available at ScienceDirect

Food Research International

journal homepage: www.elsevier.com

High resolution mass approach to characterize refrigerated black truffles stored under different storage atmospheres

Edoardo Longo[a], Ksenia Morozova[a], Monica R. Loizzo[b], Rosa Tundis[b], Sara Savini[c], Roberta Foligni[d], Massimo Mozzon[d], Daniel Martin-Vertedor[e], Matteo Scampicchio[a], Emanuele Boselli[a,*]

[a] Free University of Bozen-Bolzano, Faculty of Science and Technology, Piazza Università 1, Bozen-Bolzano, Italy
[b] Department of Pharmacy, Health and Nutritional Sciences, University of Calabria, via P. Bucci – Edificio Polifunzionale, 87036 Arcavacata di Rende (CS), Italy
[c] Chemical Safety Department, Stazione Sperimentale per l'Industria delle Conserve Alimentari (SSICA), Viale Tanara 31/a, 43100 Parma, Italy
[d] Department of Agricultural, Food and Environmental Sciences, Università Politecnica delle Marche, Via Brecce Bianche 10, 60131 Ancona, Italy
[e] Technological Institute of Food and Agriculture (CICYTEX-INTAEX), Junta of Extremadura, Avda. Adolfo Suárez s/n, 06007 Badajoz, Spain

ARTICLE INFO

Chemical compounds studied in this article:
Dehydroergosterol (PubMed CID: 6436660)
Glutathione (PubMed CID: 124886)
Adenine (PubMed CID: 190)
S-Adenosyl-homocysteine (PubMed CID: 439155)
Acetyl-carnitine (PubMed CID: 7045767)

Keywords:
Black truffle
Antioxidant power
High resolution mass spectrometry
Storage
Modified atmosphere packaging
Reduced atmospheric pressure packaging

ABSTRACT

Freshly harvested *Tuber melanosporum* samples were packed and stored at 4 °C under reduced atmospheric pressure or modified atmosphere for four weeks. Multivariate analysis was employed to correlate the antioxidant power of the ethanolic extracts of the samples with the chemical composition determined by high resolution mass spectrometry. High performance liquid chromatography coupled with a coularray detector was applied to select the chemical species associated with the antioxidant power. Four classes of chemical compounds were investigated in more detail by a targeted approach: derivatives of glutathione, adenine (such as *S*-adenosyl-homocysteine), oxidized linoleic acid and ergosterol. Adducts containing glutathione and adenine with oxidized linoleic acid were observed in TM for the first time and can be considered markers of freshness of the product. *S*-adenosyl-homocysteine, the acetyl-carnitine adduct with cysteinyl-glycine and several oxidized linoleic acid derivatives were among the markers of degradation.

1. Introduction

Tuber melanosporum (TM) is a valuable food product that can be consumed fresh or processed (Rivera, Blanco, Salvador, & Venturini, 2010). The shelf life of fresh TM can be extended by using an appropriate sealed package under reduced atmospheric pressure (hypobaric packaging) (Savini, Loizzo, Tundis, Mozzon, Foligni et al., 2017). The extraction of mycochemicals may have a strong potential for its application in the food and pharmaceutical industry. One of the most important mycochemicals is ergosterol, the primary sterol of mushrooms; ergosterol has antioxidant, anti-inflammatory and antitumor properties (Akihisa, Nakamura, Tagata, Tokuda, Yasukawa et al., 2007; Guillamón, García-Lafuente, Lozano, D'Arrigo, Rostagno et al., 2010; Villares, García-Lafuente, Guillamón, & Ramos, 2012). According to other authors, ergosterol seems to exhibit hypocholesterolemic effects, like the bioactive phytosterols (Moreno, Heleno, Barros, Barreiro, & Ferreira, 2015). Phenolic compounds of TM have been identified and quantified apparently for the first time by Villares et al. (2012). These authors obtained a phenolic extract in methanol that was characterized by HPLC after separation of proteins, organic acids, sugars and amino acids. The antioxidant properties were evaluated by inhibition of 2,2′-azobis(2-methylpropionamidine) dihydrochloride (ABAP)-induced

Abbreviations: ABTS, 2,2′-azino-bis(3-ethylbenzothiazoline-6-sulfonic acid); AMP, adenosine monophosphate; DPPH, 2,2-diphenyl-1-picrylhydrazyl; FRAP, Ferric Reducing Activity Power; GSH, glutathione; 9-HODE, (±)-9-Hydroxy-10E,12Z-octadecadienoic acid; 13-HODE, (±)-13-Hydroxy-9Z,11E-octadecadienoic acid; 9-oxoODE, 9-Oxo-10E,12Z-octadecadienoic acid; 13-oxoODE, 13-Oxo-9Z,11E-octadecadienoic acid; SAH, *S*-Adenosyl-homocysteine; SAM, *S*-Adenosyl-methionine; PCA, Principal component analysis; TM, *Tuber melanosporum*.

* Corresponding author.
Email address: emanuele.boselli@unibz.it (E. Boselli)

https://doi.org/10.1016/j.foodres.2017.09.025
Received 27 June 2017; Received in revised form 1 September 2017; Accepted 8 September 2017
Available online xxx
0963-9969/

lipid peroxidation. However, ethanolic extracts may have a wider application in the food and medicinal industry, since ethanol is food grade unlike methanol.

In this work, the whole ethanolic extract of fresh TM stored under different packaging conditions was characterized for the antioxidant compounds by means of HPLC coupled with a coularray detector. Untargeted mass spectrometric approaches have been already employed in the study of truffles (March, Richards, & Ryan, 2006) and other mushrooms (Kalogeropoulos, Yanni, Koutrotsios, & Aloupi, 2013; Miguel, Carvalho, Lourdes, Baptista, Moreira et al., 2014). The statistical analysis is exploited to direct the search of those chemical compounds related particularly to the process under study (e.g. storage, ageing) (Miguel et al., 2014). On the contrary, when the specific classes of compounds have been defined, a more detailed (targeted) approach can give useful insight on a specific aspect. Here, the compounds correlating with the loss of antioxidant capacity determined with HPLC-coularray detector were used to build up a principal component analysis (PCA) model. Successively, the antioxidant compounds significantly contributing to the variance of the PCA model were characterized with HPLC-HRMS/MS. Preliminary targeted approaches focused at studying selected chemicals (volatiles and phenolic compounds) (Savini et al., 2017). In this report, an untargeted approach aimed at probing a wide portion of the chemical species involved in the quality modifications over storage.

2. Material and methods

2.1. Chemicals and reagents

All reagents used in this study were purchased from Sigma-Aldrich S.p.A. (Milan, Italy) while solvent of analytical grade were obtained from Sigma-Aldrich S. p. A. (Milan, Italy) or VWR International s.r.l. (Milan, Italy).

2.2. Samples

Sample preparation and antioxidant assays are described elsewhere (Loizzo, Pacetti, Lucci, Núñez, Menichini et al., 2015; Savini et al., 2017). Briefly, intact fresh samples of *Tuber melanosporum* Vitt. were harvested in the hilly areas of the Marche Region (Central Italy) by a private company (Acqualagna Tartufi, PU). The fresh samples processing was reported in detail in Savini et al. (2017). The polypropylene vessels (140 × 175 × 46 mm) containing the fresh black truffles and filled with the four chosen atmospheres were sealed with an antifog polyester film adherent to a polypropylene film. The composition of the different atmospheres used were: air atmosphere (A) (control); partial vacuum (V), 0.1 bar applied; mixture of 1% O_2/99% N_2 (ON), mixture of 40% CO_2/60% N_2 (CN). Successively, the vessels were weighed, refrigerated and stored at 4 °C in the dark. Ethanolic extracts were made from these samples as described in the next section. They were investigated just at the harvesting (day 0) after 7, 14, 21 and 28 days of storage, all in triplicates.

2.3. Preparation of the extracts

An aliquot (5 g) of TM samples was weighed and blended at slow speed using a laboratory mill (M20 Universal mill, IKA®-Werke GmbH & Co. KG, Staufen, Germany). The samples were mixed with 10 ml of ethanol 96% (v/v) and were kept away from the light at room temperature for 24 h. Samples were then filtered and ethanol was newly added. The mixture was kept in the dark for other 24 h. After the second filtration, the extracts were gathered into an Erlenmeyer flask and the solvent was removed in a rotary evaporator (BUCHI Italia s.r.l). Finally, the extracts were dissolved into 5 ml of ethanol 96% (v/v). The extraction yield ranged 1.2–3.6% w/w.

2.4. Antioxidant assays

The assays were carried out previously and reported elsewhere (Loizzo et al., 2009, 2015; Savini et al., 2017). Briefly, the total antioxidant content was determined by using the Folin-Ciocalteu procedure. Each ethanolic extract was mixed with 0.2 mL Folin-Ciocalteu reagent, 2 mL of water and 1 mL of 15% Na_2CO_3. After incubation for 2 h at 25 °C the absorbance was measured at 765 nm (UV–Vis Jenway 6300 spectrophotometer, Bibby Scientific Ltd., UK). The total antioxidant content was expressed as mg GAE per g of dry extract. The $ABTS^{\cdot+}$ assay was based on the method of Loizzo, Said, Tundis, Hawas, Rashed et al. (2009). The $ABTS^{\cdot+}$ solution, produced from the reaction of ABTS 7 mM and 2.45 mM potassium persulfate, was stored in the dark at room temperature for 12 h before use and diluted with ethanol to reach an absorbance of 0.70 ± 0.05 at 734 nm. An aliquot of 25 μL of extracts at different concentrations were added to 2 mL of diluted $ABTS^{\cdot+}$ solution and the absorbance was measured after 6 min at 734 nm. Ascorbic acid was used as positive control. The radical scavenging activity was determined according to Loizzo et al. (2015). Extracts at different concentrations were added to an ethanolic solution of DPPH radical (final concentration was 0.1 mM). The bleaching of DPPH was determined by measuring the absorbance at 517 nm. Ascorbic acid was used as positive control. The chelating activity of the samples was measured following the procedure previously described elsewhere (Loizzo et al., 2009). Briefly, the extract, $FeCl_2$ (2 mM) and FerroZine™ (5 mM) were mixed and left at room temperature for 10 min. The absorbance of the Fe^{2+}-FerroZine™ complex was measured at 562 nm. The FRAP reagent, containing 2.5 mL of 10 mM tripyridyltriazine (TPTZ) solution in 40 mM HCl, 2.5 mL of 20 mM $FeCl_3$ and 25 mL of 0.3 M acetate buffer (pH 3.6) was freshly prepared. An aliquot (2.5 mg/mL) of samples was dissolved in ethanol and a 0.2 mL of this solution was mixed with 1.8 mL of FRAP reagent. Ethanol solutions of $FeSO_4$ (50–500 mM) were used to obtain the calibration curve. The absorbance of the reaction mixture was measured at 595 nm and the FRAP value was expressed as mM Fe(II)/g. Butylated hydroxytoluene (BHT) was used as positive control. DPPH, FRAP, $ABTS^{\cdot+}$ and Fe^{2+}-chelation ability are reported as IC_{50}.

2.5. Chemical composition by HPLC-HRMS and HPLC-MS/MS

2.5.1. Sample preparation

The crude ethanol extracts used for the antioxidant assays were vacuum and N_2 dried and then stored at − 80 °C. For each sample, a 50 mg/mL solution was prepared (in triplicate) in the mobile phase A of the HPLC system and vigorously stirred. No further purification was performed before injection for the LC-MS chromatographic analysis.

2.5.2. HPLC with coularray detector

The separation was carried out at a flow rate of 1 mL min^{-1} with a ODS Hypersyl C18 LC column (125 mm × 4.6 mm i.d., 5 μm, Thermo Sci.) protected with a HPLC pre-column filter (Thermo Sci.) on a Ultimate 3000 UHPLC (Thermo Sci.). The mobile phase consisted of a combination of solvent A (20 mM ammonium formate, 0.1% formic acid in water, v/v) and B (sat. ammonium formate, 0.1% formic acid in acetonitrile, v/v). The gradient was set as follows: from 5% B at 0 min to 25% B (v/v) at 21 min, then to 95% B at 22 min until 27 min, to 5% at 28 min, followed by a re-equilibration step (5% B) at 32 to 35 min. Eight porous graphite cells of the coularray detector were poised at potentials from + 300 and 860 mV (vs Pd reference electrode) with the increment of 80 mV. The data were recorded and processed with ESA

CoulArray 3.1 (Dionex) and Chromeleon software (Thermo Sci.). Retention times were corrected to match the retention time of HPLC-DAD-MS (using the retention times of injected phenolic standards employing the same LC method).

2.5.3. HPLC-DAD-HRMS analysis

The HPLC-HRMS system used consisted of a Thermo Sci. Q-Exactive HRMS instrument coupled to an Agilent 1260 HPLC with a 16 channel DAD detector. The separation was carried out at a flow rate of 1 mL min^{-1} with a ODS Hypersyl C18 LC column (125 mm × 4.6 mm i.d., 5 μm, Thermo Sci.) protected with a HPLC pre-column filter (Thermo Sci.). A contact closure electronic board allowed to interface the HPLC with the mass spectrometer. The mobile phases and the gradient were the same as for the HPLC coupled with coularray detector. The DAD recorded spectra from 210 to 600 nm and provided real-time monitoring at 280 nm (+/− 2 nm). A post-column flow splitter was used to feed both analysers in parallel (DAD and HRMS) at a fixed ratio. For Full-MS analysis, the mass spectrometer was operated parallel (polarity switch) in positive and negative ionization mode using the following conditions: sheath gas at 20 (arbitrary units), aux gas at 5 (arbitrary units), aux temperature 250 °C, spray voltage at +/− 3.5 kV, capillary temperature at 320 °C and RF S-lens at 65. The mass range selected was from 100 to 1000 *m/z* with a Full-MS set resolution of 70,000 (@200 *m/z*), AGC target at 10^6, max. Injection time of 200 ms.

2.5.4. HPLC-HRMS-dd-MS/MS analysis

Data dependent HPLC-MS/MS experiments were run in negative and positive ionization mode separately. Full-MS parameters were kept as above. MS/MS settings were: AGC target 3e5, max. Injection time 200, FTMS set resolution 17,500, loop count 5, isolation window 3 *m/z*, isolation offset 1 *m/z*, normalized collision energy 35 eV. For data dependent settings: minimum AGC target $3 \cdot 10^3$, apex trigger 2 to 8 s, charge exclusion 3–8 and higher, dynamic exclusion 10 s, "if idle" setting set to "pick others". Lock masses were included in the instrument method in both positive and negative mode. The HPLC-DAD data were collected and analysed by OpenLab software while the MS data and results were collected and analysed by Xcalibur 3.1 software and Compound Discoverer (Thermo Sci.).

2.5.5. Statistical analysis

Correlation of chemical compounds relative abundances (HPLC-MS EIC integrations) with the antioxidant activity assays was done by multivariate analysis (PCA) using Compound Discoverer and XLStat Excel package (Addinsoft, 2016.02.28430). All the variables were normalized before elaboration.

2.5.6. Screening method applied to the HRMS compound list

After the acquisition, the whole raw MS spectra dataset was processed with the software Compound Discoverer (Thermo Scientific) in both positive and negative ionization modes. No filtering constraint was applied to the compounds list, therefore only the background signals were hidden. Consequently, nearly 70,000 features (chemical compounds) in both positive and negative ionization mode were eventually identified. Therefore, we devised a procedure to reduce the analytical load, but still to retain statistical significance for the chemical species to investigate in detail. A clean-up procedure was applied to the whole datasets (Fig. 1), in order to retain only those entries in the peak list that most correlated with the change in antioxidant capacity evaluated by the antioxidant assays (Savini et al., 2017).

Firstly, a preliminary principal component analysis (PCA) was performed on the whole set of variables. The results of the antioxidant assays (ABTS (IC_{50}), DPPH (IC_{50}), FRAP values, Fe-chelating values and Folin-Ciocalteu) on all the samples were included as PCA variables. Only those features (compounds) with an index in the correlation matrix either higher than 0.4 or lower than − 0.4 were kept arbitrarily for further analysis. The result was a substantial reduction of the peak list from 70,000 to about three hundred. Furthermore, since our interest was in the chemical compound fractions displaying a relation with the antioxidant activity, an electrochemical approach was adopted. An

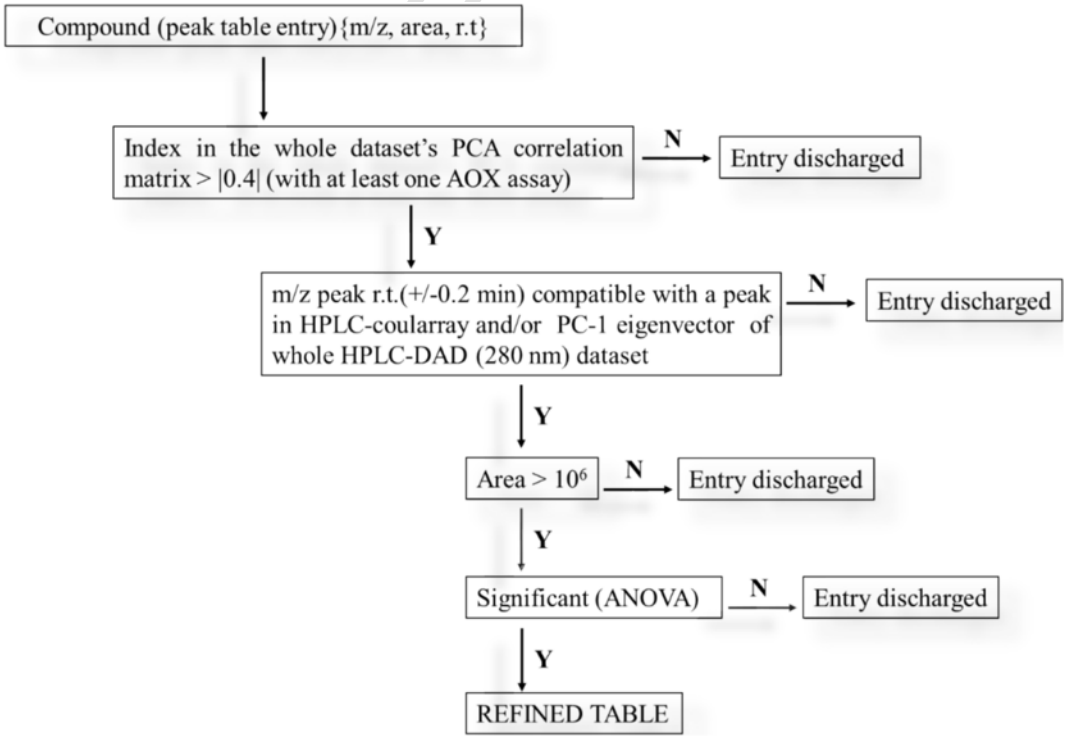

Fig. 1. Work-flow representing the steps undertaken for the preparation of the filtered sample list.

electrochemical analysis of TM samples at the beginning and in the end of the storage (CN0 and CN4) was performed. A 3D plot example of a TM analysis by HPLC with coularray detector is shown in the Fig. 2.

Coularray detection is a sensitive technique for the determination of antioxidants (Bayram, Ozcelik, Schultheiss, Frank, & Rimbach, 2013; Gamache, Meyer, Granger, & Acworth, 2004; Lijuan, Xuezhu, Haiping, & Yiru, 2007; Puspitasari-nienaber, Ferruzzi, & Schwartz, 2002; Rancan, Sabatini, Achilli, & Galletti, 2006). The highest number of peaks was detected at the coularray sensors set at + 540 and + 860 mV. Moreover, the results showed the remarkable decrease of the antioxidant species in the CN4 sample compared to CN0, which explained the decrease of the antioxidant power during the storage.

The chemical compounds absorbing at 280 nm and the compounds showing a current peak at the corresponding retention time at the cells of the coularray detector (+ 540 mV and + 860 mV) were selected from the peak lists. Aromaticity and unsaturation elicit absorption of light in the UV spectral region above 250 nm. These two traces were therefore used to build a list of peaks' retention times for filtering the MS peak list. In addition, PCA was applied on the whole HPLC-DAD dataset at 280 nm in order to select the peaks whose areas displayed a significant change over the storage period. To this purpose, the eigenvector of the first principal component was applied to this purpose; HPLC-DAD-PC1 contributed for 45.4% of total variance (see Supporting Information **Fig. SI 1** for a description). Finally, only HPLC-HRMS peaks with a retention time ± 0.2 min with respect to the HPLC-DAD-PC1 or HPLC-coularray (channels set at + 860 and + 540 mV) were retained for further investigation. Finally, the list was limited to those features with an area higher than 10^6 in at least one spectrum. ANOVA (data not shown) was then run on the refined dataset (variables) against the observations (samples) using weeks and treatments as fixed factors. The final refinement was done by removing all those table entries with no significant variance over the four weeks or by treatment as evaluated by ANOVA.

2.5.7. Qualitative compound assignment by MS/MS

MS/MS fragmentations were compared against on-line repositories (MzCloud, Mass Bank, HMDB and NIST Chemistry Webbook). Whenever data repositories were employed a reference was provided.

3. Results and discussion

The main goal of this study was to study the chemical markers associated with the modifications of TM during the shelf life study. The investigation was focused on those chemical species that showed a correlation with the loss of antioxidant power over the four weeks. The final sample lists in the negative and positive modes, obtained after these filtering steps described in Material and Methods section, are reported in Tables 1a and 1b. The table is endowed with additional information on the identified species whenever possible.

3.1. Principal component analysis of the refined datasets

The PCA of the refined datasets is presented in Fig. 3. The corresponding variables loading plots are reported in SI (**Fig. SI 2**). These PCA plots datasets differ substantially from that presented by Savini et al. (2017). In fact, the variables applied here consisted of the set of ion values obtained by untargeted HRMS analysis, whereas Savini et al.

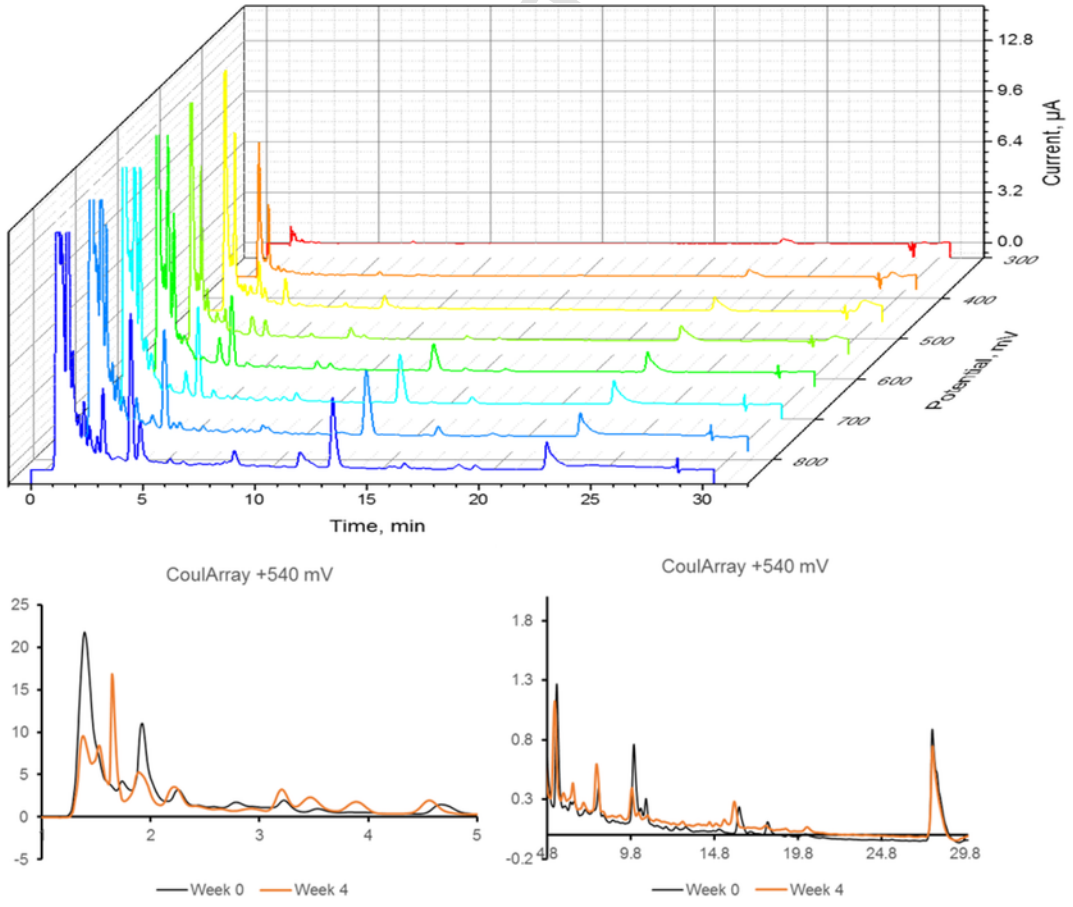

Fig. 2. Upper layer: Example of a CoulArray chromatogram for CN0. Lower layer: Comparison at CoulArray for week 0 vs week 4 (CN), showing two retention time intervals in different scale. Retention times were corrected (by injection of phenolics standards at 0 min > r.t.standard − 1 > 5 min and r.t. standard-2 > 20 min).

Table 1a
Filtered list of identified species, positive ion mode. All species were confirmed as significant by ANOVA modelling. (**) It was not possible to fully or partially assign this compound. (***) Assigned by comparison with Levison et al., 2013.

m/z	r.t.	PCA zone (*)	Ion	Charge	Neutral exact mass	Elemental composition	Tentative species or comment	Equivalent ion in negative mode (*m/z*)	Web ref.
292.1978	1.24	ZONE 3	[M + H_2O + H] + 1	1	273.3320	$C_{11}H_{23}N_5O_3$	Arg-Val dipeptide hydrate		(**5**)–(**6**)
183.0864	1.50	ZONE 0/1	[M + H] + 1	1	182.0791	$C_6H_{14}O_6$	C6-sugar alcohol (mannitol, iditol…)	181.0718, r.t. = 1.17 min (broad)	(**7**)–(**8**)
239.1025	1.89	ZONE 4	[M + NH_4] + 1	1	221.0686	$C_8H_{15}NO_6$	(**)	220.08266, r.t. = 1.89 min	
380.1486	2.42	ZONE 4	[M + H] + 1	1	379.1413	$C_{14}H_{25}O_7N_3S$	Adduct of L-Cysteinyl-Glycine with acetyl-carnitine	378.1346, r.t. = 2.48 min	(**2**)(**21**)
314.0917	3.31	ZONE 0/1	[M + H] + 1	1	313.0844	$C_{11}H_{15}O_4N_5S$	5′-*S*-Methyl-5′-thioadenosine + [O]		(**10**)
243.0992	3.41	ZONE 0/1	[M + H] + 1	1	242.0919	$C_8H_{19}O_6P$	260.12571 *m/z* = ammonium adduct, Glycerol-*n*-phosphate-C_5H_{11} (n = 1, 3)	241.0843, r.t. = 3.40 min	(**11**)
248.0587	2.59	ZONE 0/1	[M + 2FA + H_2O + H] + 1	1	137.0299	C_7H_7NS	(**)	246.0437, r.t. = 2.60 min	
298.0967	9.11	ZONE 0/1	[M + H] + 1	1	297.0894	$C_{11}H_{15}O_3N_5S$	5′-*S*-Methyl-5′-thioadenosine		(**10**)
358.1858	15.22	ZONE 0/1	[M + H] + 1	1	357.1785	$C_{18}H_{23}N_5O_3$	(**)	356.1715, r.t. = 15.21 min	
459.3064	23.67	ZONE 4	[M + H] + 1	1	458.2990	$C_{28}H_{42}O_5$	HODE derivative		(***)
455.2652	23.90	ZONE 4	[M + H] + 1	1	454.2667	$C_{24}H_{38}O_8$	HODE derivative		(***)
460.3267	23.69	ZONE 0/1	[M + H] + 1	1	459.3194	(**)	HODE derivative		(***)
441.2955	23.69	ZONE 0/1	[M + H] + 1	1	441.2725	(**)	oxoODE derivative		(***)
490.3009	23.85	ZONE 0/1	[M + H] + 1	1	489.2936	(**)	HODE derivative		(***)
432.2744	24.73	ZONE 3	[M + H] + 1	1	431.2673	(**)	HODE derivative		(***)
346.2587	24.78	ZONE 3	[M + H] + 1	1	345.2514	(**)	HODE derivative		(***)
472.2905	23.81	ZONE 0/1	[M + H] + 1	1	471.2831	(**)	HODE derivative		(***)
432.2955	23.95	ZONE 0/1	[M + H] + 1	1	431.2881	(**)	HODE derivative		(***)
385.1289	2.5	ZONE 3	[M + H] + 1	1	384.1210	$C_{14}H_{20}O_5N_6S$	*S*-adenosyl-homocysteine	383.1147, r.t. 2.48 min	(**12**)
311.2407	24.53	ZONE 0/1	[M + H] + 1	1	310.2335	$C_{21}H_{32}N_2O$	HODE + [O]		(***)

Table 1b
Filtered list of identified species, positive ion mode. All species were confirmed as significant by ANOVA modelling. (*) see main text for more information. (**) It was not possible to fully or partially assign it. (***) Assigned by comparison with Levison et al., 2013.

m/z	r.t.	PCA zone (*)	Ion	Charge	Neutral exact mass	Elemental composition	Tentative species or comment	Equivalent ion in positive mode (*m/z*)	Web ref.
473.2752	23.75	ZONE 0/1	[M-H]-1	− 1	474.2826	(**)	HODE derivative		(***)
475.2910	23.87	ZONE 0/1	[M-H]-1	− 1	476.2983	(**)	HODE derivative		(***)
159.0300	1.21	ZONE 0/1	[M-H]-1	− 1	160.0372	$C_7H_{11}O_4$	Gluconic/galactonic acid derivative		(**13**)–(**14**)
287.0536	1.25	ZONE 4	[M-H]-1	− 1	288.0607	(**)	(**)		
632.2877 (*)	23.53	ZONE 0/1	[M-H]-1	− 1	633.2950	(*)	GSH-binding HODE derivative		(**1**)-(***)
414.2320	23.95	ZONE 0/1	[M-H]-1	− 1	415.2391	(**)	HODE derivative		(***)
398.2549	23.86	ZONE 0/1	[M-H]-1	− 1	399.2620	(**)	HODE derivative		(***)
421.1649	9.83	ZONE 0/1	[M-H]-1	− 1	422.1720	$C_{17}H_{30}N_2O_8S$	Pantethine-monomer-$C_6H_8O_4$ adduct		(**15**)
423.1635	3.40	ZONE 0/1	[M-H]-1	− 1	424.1706	(**)	Glycerol-*n*-phosphate-C_5H_{11} (n = 1, 3) derivative	[M + NH_4] + adduct 260.12564 or 485.1997 *m/z* [2 M + 1] + from 243.0992 *m/z*, r.t. 3.40 min	(**11**)
483.1761	3.40	ZONE 0/1	[2M-H]-1	− 1	242.0917	$C_8H_{19}O_6P$, $[2M-1]^-$ adduct	Glycerol-*n*-phosphate-C_5H_{11} (n = 1, 3) dimer	[M + NH4] + adduct 260.12564 or 485.1997 *m/z* [2 M + 1] + from 243.0992 *m/z*, r.t. 3.40 min	(**11**)
458.3122	23.68	ZONE 0/1	[M-H]-1	− 1	459.3194	(**)	HODE derivative		(***)
573.4530	24.43	ZONE 0/1	[M-H]-1	− 1	574.4603	(**)	HODE derivative		(***)
386.1091	2.42	ZONE 0/1	[M-H]-1	− 1	387.1163	(**)	(**)		
342.0876	9.12	ZONE 0/1	[M + FA-H]-1	− 1	297.0894	$C_{11}H_{15}N_5O_3S$	Adduct 5′-*S*-Methyl-5′-thioadenosine + FA	298.0967, r.t. = 9.11 min	(**10**)
508.1807	3.36	ZONE 0/1	[M-H]-1	− 1	509.1880	(**)	Glycerol-*n*-phosphate-C_5H_{11} (n = 1, 3) derivative	[M + NH_4] + adduct 260.12564 or 485.1997 *m/z* [2 M + 1] + from 243.0992 *m/z*, r.t. 3.40 min	(**11**)
261.0876	5.84	ZONE 0/1	[M-H]-1	− 1	262.0949	$C_{13}H_{13}N_2O_4$	Asp-Phe	263.1026 *m/z*, r.t. = 5.83 min	(**16**)–(**17**)
157.0505	4.03	ZONE 0/1	[M-H]-1	− 1	158.0578	$C_7H_{10}O_4$	Isopropylmalic acid		(**18**)–(**19**)
430.2269	23.67	ZONE 0/1	[M-H]-1	− 1	431.2340	(**)	(**)	432.2407 *m/z*, r.t. = 23.60 min	
388.0707	2.49	ZONE 0/1	[M-H]-1	− 1	389.0778	(**)	Deoxyuridine derivative	390.0851, r.t. = 2.39 min	(**20**)

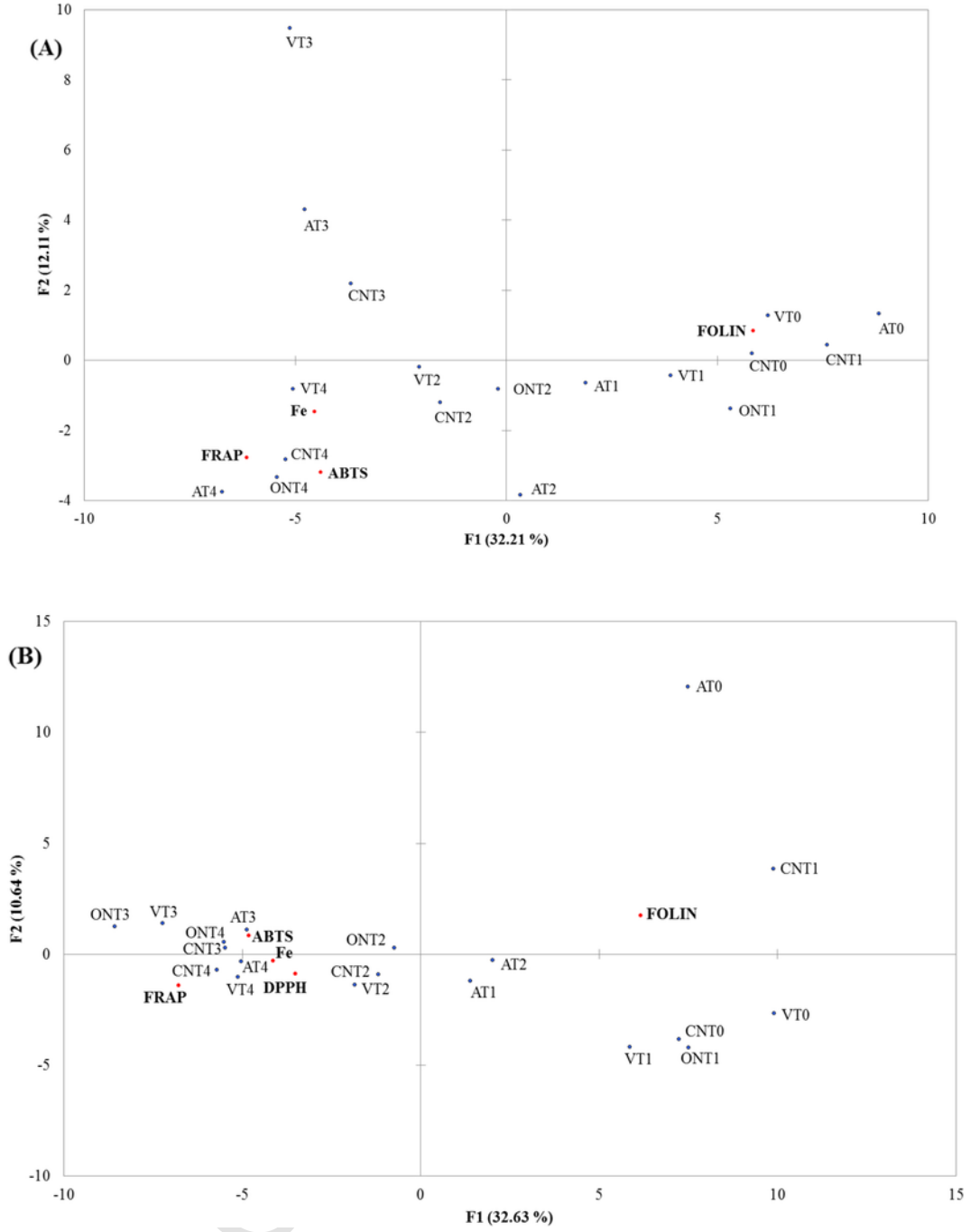

Fig. 3. (A) PCA biplot in positive ion mode on the filtered peak selection. (B) PCA biplot in negative ion mode on the filtered peak selection. Antioxidant assays distribution in the PCA are reported in SI together with the other variables.

(2017) built the model on the volatile profile evaluated by GC–MS and phenols determined by targeted analysis only.

Overall, PC-1 obtained on the reduced sample sets mirrored the effects of storage time on the samples. Besides, positive polarity analysis allowed for a better separation by week. PC-1 showed the progress of the sample degradation from positive towards negative values. The effects of PC-2 (12% of total variance) were less evident; however, PC-2 appears to separate week 3 from week 4 in positive ionization mode. ANOVA run on the refined peak list also showed no significance in the distinction between week 0 and 1 and week 1 and 2 groups, respectively. This means that an extension of the shelf life of up to two weeks could be achieved under modified atmosphere or under reduced pressure, confirming earlier results (Savini et al., 2017). Furthermore, as many compounds as possible have been identified by assigning an elemental composition and, whenever possible, a chemical structure by comparison with MS/MS fragmentation references.

3.2. *Glutathione adducts to oxidized linoleic acid derivatives*

Glutathione (GSH) is a tripeptide playing a pivotal role against oxidative stress and pathogens in organisms (Emri, Pócsi, & Szentirmai, 1997; Ghanta & Chattopadhyay, 2011; Kular, Leyland, Mejia-carranza, Reynolds, Karpinski et al., 2004; Mendoza-Cózatl, Loza-Tavera, Hernández-Navarro, & Moreno-Sánchez, 2005; Pavarino, Russo, Lívia,

Galbiatti, Almeida et al., 2013; Scharf, Remme, Habel, Chankhamjon, Scherlach et al., 2011; Zablotowicz, Hoagland, Locke, & Hickey, 1995). Several chemical compounds identified in this study can be assigned as GSH adducts. The presence of the GSH binding was proved by means of MS/MS analysis. Standard injection (**Fig. SI 3**) allowed to compare GSH MS/MS spectrum with the GSH-containing derivatives. The GSH adducts identified are reported in Table 2.

The MS/MS spectrum of 632.2878 *m/z* ($C_{31}H_{45}O_8N_4S$, see Table 1b) could not be recorded due to the presence of an overlapping contaminant. However, its exact mass corresponded to 634.3015 *m/z* (in Tables 1a and 1b) less 2H (CH-OH or CH-CH dehydrogenation/oxidation). The spectra of these GSH-containing species are reported in **Fig. SI 4**–**6**. We could assign these GSH binding species by comparison with 329.2334 *m/z*, 327.2177 *m/z* (etc.) species from the repository. Overall, only 632.2878 *m/z* appeared in the PCA filtered list, among the compounds in Table 2. The relative abundances of the GSH derivatives are shown in **Fig. SI 14** (**A**–**D**). Overall, 632.2878 *m/z* relative abundance is the highest at week 1 in normal air and carbon dioxide/nitrogen atmosphere, whereas is relatively constant in reduced pressure and reduced oxygen atmospheres.

The last entry is the product of the conjugation of a short C5 unit to GSH. The binding of short conjugated electrophiles to GSH has been already reported (Blair, 2010; Pócsi, Prade, & Penninckx, 2004). The ones among them mostly contributing to the PCA model are reported in Table 1b. Interestingly, **Fig. SI 14-D** shows that a strong increase in the concentration of this species takes place under reduced pressure (V) only at week 4. A strong similarity in the fragmentation profile was found with known oxidized linoleic acid derivatives, such as 9-HODE (Püssa, Raudsep, Toomik, Pällin, Mäeorg et al., 2009). This class of oxidized linoleic acid derivatives was already found in mushrooms (Brodowsky, Hambergi, & Oliw, 1992). They have been reported and extensively characterized (Levison, Zhang, Wang, Fu, Didonato et al., 2013; Püssa et al., 2009). In Table 3, a list of other compounds related to oxidized linoleic acid derivatives by MS/MS spectra are reported (the spectra are displayed in **Fig. SI 7**–**8** and their relative abundances in **Fig. SI 14** (**E**–**H**) and **Fig. SI 14** (**U-A1**)).

295.2273 *m/z*, also found as a MS/MS fragment of higher mass species in the list, is diagnostic for the (±)-9-hydroxy-octadecadienoic acid and (±)-13-hydroxy-octadecadienoic acid (9- and 13-HODE) according to the literature (Levison et al., 2013). Its relative abundance was relatively stable until week 3, then it displayed a decay in all tested conditions at week 4 (**Fig. SI 14-V**).

Similarly, the fragment 171.1026 *m/z* is present in all the reported MS/MS spectra and it is also found as an independent chemical species contributing to the PCA. The fragments with 171.1026, 295.2273, 311.2224 and 327.2175 *m/z* showed all an overall loss in all the tested conditions, however an initial increase was observed between week 0 and 1 in complete absence of oxygen (carbon dioxide/nitrogen atmosphere, see **Fig. SI 14** (**U**–**Y**)). The most intense of these HODE derivative compounds was 329.2334 *m/z* ($C_{18}H_{34}O_5$) and it displayed an overtime trend depending on the atmosphere used (**Fig. SI 14-Z**): whereas in normal air it smoothly increased then decreased, it grew steadily in reduced pressure (V) and reduced oxygen conditions (ON). Another oxidized analogue should be 622.4710 *m/z* whose MS/MS showed a fragment 293.212 *m/z* compatible with the presence of 9- or 13-oxy-octadecadienoic acid (9- or 13-oxoODE). Its relative abundances' plot (see **Fig. SI 14-A1**) decreased overtime but showed a very similar profile as for compounds in **Fig. SI 14** (**U**–**Y**). Consistently, linoleic acid was found as the main fatty acid also in other mushroom varieties (Levison et al., 2013). Some other identified HODE adducts in the PCA were 475.3053 *m/z* (HODE + $C_{10}H_{12}O_3$, ESI +, correspondent to negative 473.2736 *m/z*), 459.3063 *m/z* (HODE + $C_{10}H_{12}O_2$, ESI +). Tables 1a and 1b account for more of them of which not all composition could be assigned. The oxidized linoleic acid derivatives increasing over the storage time were clustered at week 3 and 4 of ESI + PCA plot and are listed in Table 1a.

Besides GSH derivatives, an adduct containing cysteinyl-glycine was found (380.1487 *m/z*) by means of MS/MS analysis in positive mode (ESI (+), $C_{14}H_{25}O_7N_3S$, Δppm = − 0.7, r.t. = 2.4 min, spectrum in

Table 2
GSH derivatives.

m/z	Retention time (min)	Associate ion	Neutral composition	Δ ppm	GSH-binding precursor in full MS spectrum	Difference from GSH in MS/MS (Δ*m/z*)	MS/MS spectra	Web ref.
634.3015	23.51	[M-H]⁻	$C_{31}H_{47}O_8N_4S$	− 1.9	327.2177	328.227	**SI 5**	**(1)**
632.2885[a]	23.52	[M-H]⁻	$C_{31}H_{45}O_8N_4S$	− 2.5	325.2012 (not found)	326.212	**N/A**	**(1)**
618.3080	23.58	[M-H]⁻	$C_{31}H_{47}O_7N_4S$	− 2.1	311.2227	312.232	**SI 6**	**(1)**
390.1341	3.80	[M-H]⁻	$C_{18}H_{22}O_4N_4S$	− 5.7	(*)	84.058	**SI 7**	**(1)**

Assignment based on MzCloud repository comparison with recorded MS/MS of L-glutathione. (*) ion out of *m/z* acquisition range.

Table 3
Linoleic acid oxidized derivatives.

m/z	Retention time (min)	Associate ion	Neutral composition	Δ ppm	MS/MS spectra
639.4496	24.22, 24.59, 25.01	[M-H]⁻	$C_{36}H_{64}O_9$	1.9	**SI 8**
623.4528	24.22, 24.77, 25.69	[M-H]⁻	$C_{36}H_{64}O_8$	1.6	**SI 8**
605.4429	25.42, 26.43	[M-H]⁻	$C_{36}H_{62}O_7$	1.0	**SI 8**
589.4471	25.91	[M-H]⁻	$C_{36}H_{62}O_6$	− 0.5	**SI 8**
171.1026[a]	21.47, 21.97, 23.58, 24.21	[M-H]⁻	$C_9H_{16}O_3$	− 0.2	**SI 7**
295.2276	24.41	[M-H]⁻	$C_{18}H_{32}O_3$	− 0.8	**SI 7**
311.2227	24.21	[M-H]⁻	$C_{18}H_{32}O_4$	− 0.3	**SI 7**
327.2175	24.21	[M-H]⁻	$C_{18}H_{32}O_5$	− 0.2	**SI 7**
329.2331	23.76	[M-H]⁻	$C_{18}H_{34}O_5$	− 0.7	**SI 7**

Assignment based on MzCloud repository comparison with recorded MS/MS.
[a] Significant by ANOVA.

Fig. SI 9). The presence of Cys-Gly was confirmed by MS/MS comparison on MzCloud (web ref. 2). Its relative abundance (**Fig. SI 14-Q**) increased steadily in all conditions and could be regarded as another marker of degradation. This adduct contributed significantly to the PCA. The identity of the fragment coupled to Cys-Gly was tentatively assigned to acetyl-carnitine ($C_9H_{18}O_4N$, $[M]^+ = 204.1230$ *m/z*), a positively charged natural compound that was also found in the samples (web ref. 21, see MS/MS in **Fig. SI 15** and relative abundance change at **Fig. SI 14-A2**). It showed an increasing trend over the storage time (**Fig. SI 14-A2**) analogous to its adduct with cysteinyl-glycine. Acetyl-L-carnitine was already found in mushrooms (Knüttel-Gustavsen & Harmeyer, 2007) and its consumption has been associated to several metabolic and clinical effects in human (Bremer, 1983).

3.3. Adenine-containing derivatives

Adenine is an electron-rich compound which has shown the ability to lose up to six electrons in water-mediated oxidation (Gonçalves, Batchelor-Mcauley, Barros, & Compton, 2010). Several adenine containing compounds that contributed to the PCA were identified in the samples in positive ionization mode. Their identification was possible by comparison of the MS/MS pattern with the repository by 136.0626 *m/z* fragment (ESI (+), $C_5H_5N_5$, adenine ring). Adenosine itself was identified (**Fig. SI 10**) and other derivatives of adenine are reported in Table 4.

Very interestingly, the parent ion at 448.2912 *m/z* (**Fig. SI 11**) differs from adenine by 312.2296 *m/z* which corresponds to one of the observed oxidized linoleic acid (HODE) species in negative ion mode (311.2227 *m/z*). Notably, adenine forms adducts with epoxide and carbonyl derivatives (Carmical, Zhang, Nechev, Harris, Harris et al., 2000; Carmical, Nechev, Harris, Harris, & Lloyd, 2000; Chang, Seneviratne, Wu, Tretyakova, & Essigmann, 2017; Lee, Ringer, Bible, Hajdu, & Blair, 2000). In particular, it was shown that adenine forms adducts with 4-oxo-nonenal, an aldehyde similar to those found in the volatile profile of TM (Savini et al., 2017). Besides, some adenine adducts decreased during the storage and showed into the refined list used in the PCA, such as *S*-methyl-thioadenosine (see relative abundance trends in **Fig. SI 14-M**). Interestingly, also *S*-adenosyl-homocysteine (SAH) was identified (**Fig. SI 12**) but it appeared to increase overtime (until week 3 in normal atmosphere and till week 4 in all other conditions, **Fig. SI 14-K**. SAH is produced as a by-product of the DNA transmethylation from the precursor *S*-adenosyl-methionine (SAM) (Lu, 2000). SAH is also a precursor for the synthesis of glutathione via L-cysteine formation.

3.4. Ergosterol and its derivatives

Dehydroergosterol ($[M + H]^+ = 395.3306$ *m/z*, **Fig. SI 13**) and two other ergosterol derivatives were observed and listed in Table 5.

Only traces were found of ergosterol ($[M + H]^+ = 397.3465$ *m/z*). NIST Chemistry Webbook online was used for the assignment, still the reported reference spectrum of ergosterol had been acquired by EI-MS, therefore the molecular ion showed a *m/z* value of 396. However, the loss of one water molecule was observed in the ergosterol reference MS/MS spectrum. Few other reports investigated ergosterol and its derivatives by HRMS/MS analysis although none of them showed the MS/MS fragmentation in conditions close enough for a definitive comparison. As observed earlier with GC–MS and GC–MS/MS, this whole class of compounds shows the characteristic loss of one water molecule (Headley, 2002; Varga, 2006), and this aided the identification. The MS/MS spectra of these chemical species are reported in **Fig. SI 13**. Their relative abundances are reported in **Fig. SI 14 R-T**. In MS/MS, several common peaks were found for this group (e.g. 55.055, 67.055, 69.070, 79.055, 93.070, 95.056, 97.101, 109.076, 117.070 *m/z*). All the parents observed appears to be related to 395.3308 *m/z*. However, none of those confirmed or identified contributed to the PCA.

4. Conclusions

An untargeted approach allowed to identify and characterize a wide selection of chemical components involved in the modifications of fresh *Tuber melanosporum* during the refrigerated storage in vessels packed under different atmospheres. These compounds were statistically correlated, directly or inversely, with the loss of antioxidant activity and in general with the metabolism of TM. The metabolic activity of TM was demonstrated to endure over the storage up to two weeks (Rivera et al., 2010). Moreover, the results were in agreement with previous findings of a shelf-life study on the evolution of volatiles, the loss of antioxidant power measured by various assays and the phenolics profile (Savini et al., 2017). The present work addressed a much different and wider range of chemical classes, giving a detailed overview of the TM metabolism under storage in normal or modified atmosphere packaging. The presence of adenine, ergosterol and glutathione derivatives were discussed in detail. Adenine and GSH are electron-rich species that have been known to couple to electrophyles and intervene in oxidation protection processes. In particular, the formation of adducts of adenine and GSH with the same oxidized linoleic acid derivatives was observed for the first time in TM. Interestingly, they showed to bind to an oxidation derivative of linoleic acid already reported in mushrooms (Levison et al., 2013). These adducts may also be related to the formation of off-flavors both from degradation of the lipid fraction (e.g. HODE) and from sulfur containing precursors (e.g. GSH, Cys-Gly, *S*-adenosyl-homocysteine etc.). Besides, derivatives of dehydroergosterol were detected by MS/MS comparison of identified species with the repositories Another group of compounds was also identified and completely or partially assigned, such as C6 sugar alcohols (Table 1a). Some among them also correlated with the loss of antioxidant capacity (as shown by PCA). Others were growing over the storage, so they inversely correlated with the total antioxidant power loss (for example, *S*-adenosyl-homocysteine, the Cys-Gly adduct with acetyl-carnitine and several oxidized linoleic acid derivatives). The contribution of these adducts to the overall antioxidant capacity change may be related to the metabolic response of TM in order to cope with the stress induced by the storage conditions. This means that an extension of the shelf life up to two weeks could be achieved under modified atmosphere or under reduced pressure confirming a recent report (Savini et al., 2017). In fact, ANOVA run on the refined list also showed no significance in the distinction between week 0 and 1 and week 1 and 2, respectively. Overall, the use of reduced atmospheric pressure proved to be a viable and cheaper alternative to modified atmospheres.

Conflict of interests

The authors declare that they have no conflict of interest.

Acknowledgement

Funding institutions were Regione Marche (Italy) (DDS n. 631, 06/11/2012, Progetto integrato di microfiliera El Tartuf) and Province of Bolzano (Italy) (Landesregierung mittels Beschluss Nr. 1472, 07.10.2013). The authors would also like to thank Acqualagna Tartufi for their kind assistance in providing and preparing the truffles.

Compliance with ethic requirements

All authors declare that this article does not contain any studies with human or animal subjects.

Table 4
Adenine derivatives.

m/z	Retention time (min)	Associate ion	Neutral composition	Δ ppm	Difference from (adenine) 136.062 *m/z* in MS/MS spectrum	MS/MS spectra	Correspondent in negative mode ([M-H]$^-$)	Web ref.
448.2912	23.96	[M + H]$^+$	$C_{23}H_{37}O_4N_5$	− 1.4	312.230	**SI 11**	446.2773 *m/z*, r.t. 23.97 min	(**3**)
413.1415	7.49	[M + H]$^+$	(**)		277.080	**SI 11**	411.1269 *m/z*, r.t. 7.49 min	(**3**)
385.1289	2.5	[M + H]$^+$	*S*-adenosyl-homocysteine, $C_{14}H_{20}O_5N_6S$	− 0.4	249.066	**SI 12**	383.1147, r.t. 2.48 min	(**3**)
348.1915	1.30	[M + H]$^+$	5′- or 3′-adenosine-monophosphate AMP), $C_{10}H_{14}O_7N_5P$	0.1	212.115	**SI 12**	346.0558, r.t. 1.30 min	(**9**)
314.0917[a]	3.31	[M + H]$^+$	5′-*S*-methyl-thioadenosine + [O], $C_{11}H_{15}O_4N_5S$	− 0.3	178.030	**SI 11**	312.0948, r.t. 3.24 min	(**3**)
298.0968[a]	9.04	[M + H]$^+$	5′-*S*-methyl-thioadenosine, $C_{11}H_{15}O_3N_5S$	0.0	162.035	**SI 11**	296.0823, r.t. 9.04 min	(**3**)
252.1086	4.10	[M + H]$^+$	deoxyadenosine/cordycepin, $C_{10}H_{13}O_3N_5$	− 2.5	116.046	**SI 11**	250.0930, r.t. 4.13 min	(**3**)
250.0932	5.54	[M + H]$^+$	deoxyadenosine – [2H], $C_{10}H_{11}O_3N_5$	− 1.1	114.031	**SI 11**	NF	(**3**)

(*) from adenine in MS/MS spectrum. Assignment based on MzCloud repository comparison with recorded MS/MS. (**) not completely assigned.
[a] Significant by ANOVA.

Table 5
Ergosterol derivatives.

m/z	Retention time (min)	Associate ion	Neutral composition (tentative)	Δ ppm	Comment	MS/MS spectra	Web ref.
397.3465	26.96	$[M + H]^+$	$C_{28}H_{44}O$	− 0.35	Ergosterol	**NA**	(4)
395.3306	28.11	$[M + H]^+$	$C_{28}H_{42}O$	− 0.61	Dehydroergosterol	**SI 13**	(4)
586.4460	28.91	(**)	(**)	(**)	(**)	**SI 13**	(4)
412.3056	24.09	(**)	(**)	(**)	(**)	**SI 13**	(4)

Appendix A. Supplementary data

Supplementary data to this article can be found online at http://dx.doi.org/10.1016/j.foodres.2017.09.025.

References

Akihisa, T., Nakamura, Y., Tagata, M., Tokuda, H., Yasukawa, K., Uchiyama, E., … Kimura, Y., 2007. Anti-inflammatory and anti-tumor-promoting effects of triterpene acids and sterols from the fungus Ganoderma lucidum. Chemistry and Biodiversity 4 (2), 224–231, (http://dx.doi.org/10.1002/cbdv.200790027).

Bayram, B., Ozcelik, B., Schultheiss, G., Frank, J., Rimbach, G., 2013. A validated method for the determination of selected phenolics in olive oil using high-performance liquid chromatography with coulometric electrochemical detection and a fused-core column. Food Chemistry 138 (2–3), 1663–1669, (http://dx.doi.org/10.1016/j.foodchem.2012.11.122).

Blair, I.A., 2010. Analysis of endogenous glutathione-adducts and their metabolites. Biomedical Chromatography 24 (1), 29–38, (http://dx.doi.org/10.1002/bmc.1374).

Bremer, J., 1983. Carnitine - metabolism and functions. Physiological Reviews 63 (4), 1420–1480.

Brodowsky, I.D., Hambergi, M., Oliw, E.H., 1992. A linoleic acid (8R)-dioxygenase and hydroperoxide isomerase of the fungus Gaeumannomyces graminis. Biochemistry 267 (21), 14738–14745.

Carmical, J.R., Nechev, L.V., Harris, C.M., Harris, T.M., Lloyd, R.S., 2000. Mutagenic potential of adenine N6 adducts of monoepoxide and diolepoxide derivatives of butadiene. Environmental and Molecular Mutagenesis 35 (1), 48–56, (https://doi.org/10.1002/(SICI)1098-2280(2000)35:1 < 48::AID-EM7 > 3.0.CO;2-C).

Carmical, J.R., Zhang, M., Nechev, L., Harris, C.M., Harris, T.M., Lloyd, R.S., 2000. Mutagenic potential of guanine N2 adducts of butadiene mono- and diolepoxide. Chemical Research in Toxicology 13 (1), 18–25, (http://dx.doi.org/10.1021/tx9901332).

Chang, S., Seneviratne, U.I., Wu, J., Tretyakova, N., Essigmann, J.M., 2017. 1,3-butadiene-induced adenine DNA adducts are genotoxic but only weakly mutagenic when replicated in Escherichia coli of various repair and replication backgrounds. Chemical Research in Toxicology(acs.chemrestox.7b00064. http://dx.doi.org/10.1021/acs.chemrestox.7b00064).

Emri, T., Pócsi, I., Szentirmai, A., 1997. Glutathione metabolism and protection against oxidative stress. Free Radical Biology & Medicine 23 (5), 809–814.

Gamache, P.H., Meyer, D.F., Granger, M.C., Acworth, I.N., 2004. Metabolomic applications of electrochemistry/mass spectrometry. Journal of the American Society for Mass Spectrometry 15 (12), 1717–1726, (http://dx.doi.org/10.1016/j.jasms.2004.08.016).

Ghanta, S., Chattopadhyay, S., 2011. Glutathione as a signaling molecule - another challenge to pathogens. Plant Signaling & Behavior 6 (6), 783–788, (http://dx.doi.org/10.4161/psb.6.6.15147).

Gonçalves, L.M., Batchelor-Mcauley, C., Barros, A.A., Compton, R.G., 2010. Electrochemical oxidation of adenine: A mixed adsorption and diffusion response on an edge-plane pyrolytic graphite electrode. Journal of Physical Chemistry C 114 (33), 14213–14219, (http://dx.doi.org/10.1021/jp1046672).

Guillamón, E., García-Lafuente, A., Lozano, M., D'Arrigo, M., Rostagno, M.A., Villares, A., Martínez, J.A., 2010. Edible mushrooms: Role in the prevention of cardiovascular diseases. Fitoterapia 81 (7), 715–723, (http://dx.doi.org/10.1016/j.fitote.2010.06.005).

Kalogeropoulos, N., Yanni, A.E., Koutrotsios, G., Aloupi, M., 2013. Bioactive microconstituents and antioxidant properties of wild edible mushrooms from the island of Lesvos, Greece. Food and Chemical Toxicology 55, 378–385, (http://dx.doi.org/10.1016/j.fct.2013.01.010).

Knüttel-Gustavsen, S., Harmeyer, J., 2007. The determination of L-carnitine in several food samples. Food Chemistry 105, 793–804, (http://dx.doi.org/10.1016/j.foodchem.2007.01.058).

Kular, B., Leyland, N., Mejia-carranza, J., Reynolds, H., Karpinski, S., Mullineaux, P.M., 2004. Evidence for a direct link between glutathione biosynthesis and stress defense gene expression in Arabidopsis. The Plant Cell 16 (September), 2448–2462, (http://dx.doi.org/10.1105/tpc.104.022608.1).

Lee, S.H., Ringer, D., Bible, R.H.J., Hajdu, E., Blair, I.A., 2000. Characterization of 2′-deoxyadenosine adducts derived from 4-oxo-2-nonenal, a novel product of lipid peroxidation. Chemical Research in Toxicology 13 (7), 565–574, http://dx.doi.org/10.1021/tx000057z. (CCC).

Levison, B.S., Zhang, R., Wang, Z., Fu, X., Didonato, J.A., Hazen, S.L., 2013. Quantification of fatty acid oxidation products using online high-performance liquid chromatography tandem mass spectrometry. Free Radical Biology and Medicine 59, 2–13, (http://dx.doi.org/10.1016/j.freeradbiomed.2013.03.001).

Lijuan, M., Xuezhu, Z., Haiping, Z., Yiru, G., 2007. Development of a fingerprint of Salvia miltiorrhiza Bunge by high-performance liquid chromatography with a coulometric electrode array system. Journal of Chromatography B: Analytical Technologies in the Biomedical and Life Sciences 846 (1–2), 139–146, (http://dx.doi.org/10.1016/j.jchromb.2006.08.048).

Loizzo, M.R., Pacetti, D., Lucci, P., Núñez, O., Menichini, F., Frega, N.G., Tundis, R., 2015. Prunus persica var. platycarpa (Tabacchiera Peach): Bioactive compounds and antioxidant activity of pulp, peel and seed ethanolic extracts. Plant Food for Human Nutrition 70 (3), 331–337.

Loizzo, M.R., Said, A., Tundis, R., Hawas, U.W., Rashed, K., Menichini, F., … Menichini, F., 2009. Antioxidant and antiproliferative activity of Diospyros lotus L. extract and isolated compounds. Plant Food for Human Nutrition 64, 264–270.

Lu, S.C., 2000. S-adenosylmethionine. The International Journal of Biochemistry & Cell Biology 32 (4), 391–395, (http://dx.doi.org/10.1016/S1357-2725(99)00139-9).

March, R.E., Richards, D.S., Ryan, R.W., 2006. Volatile compounds from six species of truffle - head-space analysis and vapor analysis at high mass resolution. International Journal of Mass Spectrometry 249–250, 60–67, (http://dx.doi.org/10.1016/j.ijms.2005.12.038).

Mendoza-Cózatl, D., Loza-Tavera, H., Hernández-Navarro, A., Moreno-Sánchez, R., 2005. Sulfur assimilation and glutathione metabolism under cadmium stress in yeast, protists and plants. FEMS Microbiology Reviews 29 (4), 653–671, (http://dx.doi.org/10.1016/j.femsre.2004.09.004).

Miguel, L., Carvalho, F., Lourdes, M.D., Baptista, P., Moreira, N., Rita, A., … Pinho, D., 2014. Non-targeted and targeted analysis of wild toxic and edible mushrooms using gas chromatography – ion trap mass spectrometry. Talanta 118, 292–303, (http://dx.doi.org/10.1016/j.talanta.2013.09.038).

Moreno, A., Heleno, S.A., Barros, L., Barreiro, M.F., Ferreira, I.C.F.R., 2015. 2nd symposyum on medicinal chemistry. In: Antioxidant activity of Agaricus bisporus L. hexane and ethanol extracts obtained by Soxhlet and ultrasound-assisted extraction: The importance ofthe presence of ergosterol. pp. 1–2.

Pavarino, É.C., Russo, A., Lívia, A., Galbiatti, S., Almeida, W.P., Goloni Bertollo, E.M., 2013. Glutathione: Biosynthesis and mechanism of action. In: Labrou, N., Flemetakis, E. (Eds.), Glutathione: Biochemistry, mechanism of action and biotechnological implication. Nova Science Ed.

Pócsi, I., Prade, R.A., Penninckx, M.J., 2004. Glutathione, altruistic metabolite in fungi. Advances in Microbial Physiology 49 (1), 1–76, (http://dx.doi.org/10.1016/S0065-2911(04)49001-8).

Puspitasari-nienaber, N.L., Ferruzzi, M.G., Schwartz, S.J., 2002. Simultaneous detection of tocopherols, carotenoids and chlorophylls in vegetable oils by direct injection C30 RP-HPLC with coulometric electrochemical array detection. Journal of the American Oil Chemists Society 79 (7), 633–640, (http://dx.doi.org/10.1007/s11746-002-0536-0).

Püssa, T., Raudsepp, P., Toomik, P., Pällin, R., Mäeorg, U., Kuusik, S., … Rei, M., 2009. A study of oxidation products of free polyunsaturated fatty acids in mechanically deboned meat. Journal of Food Composition and Analysis 22 (4), 307–314, (http://dx.doi.org/10.1016/j.jfca.2009.01.014).

Rancan, M., Sabatini, A.G., Achilli, G., Galletti, G.C., 2006. Determination of imidacloprid and metabolites by liquid chromatography with an electrochemical detector and post column photochemical reactor. Analytica Chimica Acta 555 (1), 20–24, (http://dx.doi.org/10.1016/j.aca.2005.08.058).

Rivera, C.S., Blanco, D., Salvador, M.L., Venturini, M.E., 2010. Shelf-life extension of fresh Tuber aestivum and Tuber melanosporum truffles by modified atmosphere packaging with microperforated films. Journal of Food Science 75 (4), (http://dx.doi.org/10.1111/j.1750-3841.2010.01602.x).

Savini, S., Loizzo, M.R., Tundis, R., Mozzon, M., Foligni, R., Longo, E., … Boselli, E., 2017. Fresh refrigerated Tuber melanosporum truffle: Effect of the storage conditions on the antioxidant profile, antioxidant activity and volatile profile. European Food Research and Technology 1–9, (http://dx.doi.org/10.1007/s00217-017-2927-x).

Scharf, D.H., Remme, N., Habel, A., Chankhamjon, P., Scherlach, K., Heinekamp, T., … Hertweck, C., 2011. A dedicated glutathione S-transferase mediates carbon-sulfur bond formation in gliotoxin biosynthesis. Journal of the American Chemical Society 133 (32), 12322–12325, (http://dx.doi.org/10.1021/ja201311d).

Villares, A., García-Lafuente, A., Guillamón, E., Ramos, , 2012. Identification and quantification of ergosterol and phenolic compounds occurring in Tuber spp. truffles. Journal of Food Composition and Analysis 26 (1–2), 177–182, (http://dx.doi.org/10.1016/j.jfca.2011.12.003).

Zablotowicz, R.M., Hoagland, R.E., Locke, M.a., Hickey, W.J., 1995. Glutathione-S-transferase activity and metabolism of glutathione conjugates by rhizosphere bacteria, 61(3). 1054–1060.

Web references

Ergosterol. Repository: NIST Mass Spectrometry Data Center. Origin: Japan AIST/NIMC Database – Spectrum MS-NW-1727. NIST MS Number: 229095. http://webbook.nist.gov/cgi/cbook.cgi?ID=C57874&Mask=200#Top.

Gluconic acid. Repository: MzCloud. Year: 2014. Contributor: Tim Stratton (Thermo Fisher Scientific, San Jose, CA, USA). Curator: Andrea Belicova (HighChem, Bratislava, Slovakia). https://www.mzcloud.org/DataViewer#Creference1226.

2′-Deoxyuridine. Repository: MzCloud. Year: 2014. Contributor: Eric Genin (Thermo Fisher Scientific, Villebon-sur-Yivette, France). Curator: Alena Bednarikova (HighChem, Bratislava, Slovakia). https://www.mzcloud.org/DataViewer#Creference140.

Glycerol 3′-phosphate. Repository: MzCloud. Year: 2014. Contributor: Eric Genin (Thermo Fisher Scientific, Villebon-sur-Yivette, France). Curator: Alena Bednarikova (HighChem, Bratislava, Slovakia). https://www.mzcloud.org/DataViewer#Creference1489.

Mannitol. Repository: MzCloud. Year: 2015. Contributor: Eric Genin (Thermo Fisher Scientific, Villebon-sur-Yivette, France). Curator: Alena Bednarikova (HighChem, Bratislava, Slovakia). https://www.mzcloud.org/DataViewer#Creference1501.

Galactonic acid. Repository: MzCloud. Year: 2014. Contributor: Eric Genin (Thermo Fisher Scientific, Villebon-sur-Yivette, France). Curator: Alena Bednarikova (HighChem, Bratislava, Slovakia). https://www.mzcloud.org/DataViewer#Creference1530.

2-Isopropylmalic acid. Repository: MzCloud. Year: 2014. Contributor: Eric Genin (Thermo Fisher Scientific, Villebon-sur-Yivette, France). Curator: Alena Bednarikova (HighChem, Bratislava, Slovakia). https://www.mzcloud.org/DataViewer#Creference154.

Adenosine 5′-monophosphate. Repository: MzCloud. Year: 2014. Contributor: Eric Genin (Thermo Fisher Scientific, Villebon-sur-Yivette, France). Curator: Alena Bednarikova (HighChem, Bratislava, Slovakia). https://www.mzcloud.org/DataViewer#Creference194.

3-Isopropylmalic acid. Repository: MzCloud. Year: 2014. Contributor: Eric Genin (Thermo Fisher Scientific, Villebon-sur-Yivette, France). Curator: Alena Bednarikova (HighChem, Bratislava, Slovakia). https://www.mzcloud.org/DataViewer#Creference204.

5′- *S*-Methyl-5′-thioadenosine. Repository: MzCloud. Year: 2014. Contributor: Eric Genin (Thermo Fisher Scientific, Villebon-sur-Yivette, France). Curator: Alena Bednarikova (HighChem, Bratislava, Slovakia). https://www.mzcloud.org/DataViewer#Creference253.

Iditol. Repository: MzCloud. Year: 2015. Contributor: Tim Stratton (Thermo Fisher Scientific, San Jose, CA, USA). Curator: Jana Semanova (HighChem, Bratislava, Slovakia). https://www.mzcloud.org/DataViewer#Creference2573.

Adenine. Repository: MzCloud. Year: 2015. Contributor: Eric Genin (Thermo Fisher Scientific, Villebon-sur-Yivette, France). Curator: Alena Bednarikova (HighChem, Bratislava, Slovakia). https://www.mzcloud.org/DataViewer#Creference296.

L-Arginine. Repository: MzCloud. Year: 2015. Contributor: Rachel Norton (Thermo Fisher Scientific, San Jose, CA, USA). Curator: Jana Semanova (HighChem, Bratislava, Slovakia). https://www.mzcloud.org/DataViewer#Creference2977.

Cysteinylglycine. Repository: MzCloud. Year: 2015. Contributor: Eric Genin (Thermo Fisher Scientific, Villebon-sur-Yivette, France). Curator: Alena Bednarikova (HighChem, Bratislava, Slovakia). https://www.mzcloud.org/DataViewer#Creference363.

D-Panthetine. Repository: MzCloud. Year: 2015. Contributor: Eric Genin (Thermo Fisher Scientific, Villebon-sur-Yivette, France). Curator: Alena Bednarikova (HighChem, Bratislava, Slovakia). https://www.mzcloud.org/DataViewer#Creference416.

L-Aspartic acid. Repository: MzCloud. Year: 2015. Contributor: Eric Genin (Thermo Fisher Scientific, Villebon-sur-Yivette, France). Curator: Alena Bednarikova (HighChem, Bratislava, Slovakia). https://www.mzcloud.org/DataViewer#Creference462.

L-Glutathione (reduced). Repository: MzCloud. Year: 2015. Contributor: Eric Genin (Thermo Fisher Scientific, Villebon-sur-Yivette, France). Curator: Alena Bednarikova (HighChem, Bratislava, Slovakia). https://www.mzcloud.org/DataViewer#Creference472.

***S*-Adenosyl-homocysteine**. Repository: MzCloud. Year: 2016. Contributor: Eric Genin (Thermo Fisher Scientific, Villebon-sur-Yivette, France). Curator: Alena Bednarikova (HighChem, Bratislava, Slovakia). https://www.mzcloud.org/DataViewer#Creference592.

L-Valine. Repository: MzCloud. Year: 2015. Contributor: Eric Genin (Thermo Fisher Scientific, Villebon-sur-Yivette, France). Curator: Alena Bednarikova (HighChem, Bratislava, Slovakia). https://www.mzcloud.org/DataViewer#Creference772.

L-Phenylalanine. Repository: MzCloud. Year: 2015. Contributor: Tim Stratton (Thermo Fisher Scientific, San Jose, CA, USA). Curator: Jana Semanova (HighChem, Bratislava, Slovakia). https://www.mzcloud.org/DataViewer#Creference8.

Acetyl-L-carnitine. Repository: MzCloud. Year: 2017. Contributor: Andrea Belicova, Jana Semanova. (Thermo-Fisher Scientific/High-Chem). Curator: Alena Bednarikova (HighChem, Bratislava, Slovakia) https://www.mzcloud.org/DataViewer#Creference879#T10468#c.